Modelling of nanoindentation to simulate thin layer behaviour

R. MAJOR[1], P. LACKI[2], J.M. LACKNER[3], and B. MAJOR[1*]

[1] Institute of Metallurgy and Materials Science, Polish Academy of Sciences, 25 Reymonta St., 30-059 Cracow, Poland
[2] Czestochowa University of Technology, 19 Armii Krajowej Ave, 42-200 Czestochowa, Poland
[3] Joanneum Research Forschungsgesellschaft, Laser Center Leoben, A-8712 Niklasdorf, Austria

Abstract. The work presents a computer simulation realized with the ADINA program concerning nanoindendation test. A shape of nanoindenter was proposed to be similar to the real surgical tools. The theoretical model was used to predict phenomena which would appear in practice. The contribution of the TiN coating thickness to the implant rigid properties was simulated. Three types of extortion conditions could be considered, i.e., short contact with surgery tool (i); long continuous contact with natural tissue (ii); long cyclic contact with natural tissue (iii). In the first part of the work, the authors focused on the first type of extortion (i). The second part of the work is dedicated to the calculations of temperature impact to layer behaviour. Two layer thicknesses are considered i.e., 250 nm and 50 nm. The examined coatings find serious practical applications as a blood-contacting material in medicine. The coatings were subjected to transmission electron microscopy investigations. Columnar mechanism of film growth controlled by kinetic process is stated to operate for the considered range of layer thickness. Plasma temperature is observed to influence the substrate behaviour. Examinations of thinner layers, i.e. under 100nm, revealed higher degree of smoothness and uniformity, which could be related to the operation of the surface diffusion mechanism at the early stage of deposition. The physical explanation of TEM images was based on the finite element calculations of the temperature distribution using the ADINA program .

Key words: nanoindentation, finite element modelling, temperature, stress, strain, thin layers.

1. Introduction

Segmented polyurethane (PU) is seen as a nominal bio-material for clinical applications [1]. This is due to the excellent combination of mechanical and elastic properties with bio-compatibility. However, the fact of micro-thrombosis formation in vivo environment and control of wettability makes it necessity to apply the processes of surface engineering to modify the surface of implants. It is crucial especially in the case of internal implantation. Pulsed laser deposition (PLD) could be selected to deposit titanium nitride (TiN) on PU due to possible deposition without PU substrate heating, leading to thermal degradation [2,3]. The formation of the hard and brittle ceramic TiN coating can influence the rigid properties of the bulk material and the physico-chemical properties. They are related to the thickness of the deposited layer. It is necessary to apply an optimal thickness which does not diminish the rigidity of the device but enhances its behaviour in the biological environment.

The finite-element method has gained a growing popularity among the numerical techniques in engineering [4]. Firstly, this is because the engineering design of modern products requires an engineer to predict accurately the performance and produce the optimal object, which requires an integrated use of the finite-element analysis software in CAD. Secondly, fast progress in hardware performance and a great decrease in the price of computers offer the possibility of using finite-element analysis software. Another important factor is that the analysis functions of the finite-elements program themselves develop rapidly, offering a user-friendly interface and CAD software [5].

In recent years, nanoindentation techniques have been used to determine the hardness and Young's modulus of thin films [6]. Indentation hardness measurements are now extensively used for characterization and ranking of coated systems for mechanical applications because they are simple, cheap and reproducible [7]. However, the presence of the underlying substrate, including the interface of material, may complicate the interpretation of measurement results. Owing to a gradually increasing influence of the substrate, the hardness of composite systems depends possibly not only on coating material, but also on coating thickness and substrate hardness. The impact of the substrate on the hardness of composite systems is also transferred by an interaction that occurs at the interface. While discussing the interface influence, it is difficult to obtain detailed information experimentally, such as deformation behaviour and stress and strain distribution inside the coated systems, especially near the interface. Up to now, not much work has been done dealing with the influence of the interface strength between coating and substrate on the indentation process of coated systems. It is well known that the finite-element method (FEM) can handle the infinite continuum problem as a discrete approximation and give a dynamic insight into deformation process as well as yield important values which are difficult to obtain in experiments. The current work follows and develops the idea initiated by the authors in [8] and deals with a problem of physical verification of the calculation as well as distribution of temperature in the layer and in the substrate as well. In the case of the second part of the work, the FEM was used to explain the physical phenomena observed by transmission electron microscopy as well as to simulate a new composition of the layers.

---

*e-mail: nmmajor@imim-pan.krakow.pl

The goal of this work is to simulate the thin layer properties established by different nanoindenter treatments and the temperature influence onto the layer substrate interaction.

1.1. Growth modes. Depending on the thickness of the deposited layer it is possible to classify the models of the film growth operating at the early and late stage of deposition [2,3,9,10]. In the Frank-van der Merwe (FM) mode, a single crystal layer covers the substrate uniformly. This is the configuration suitable for most applications, but unfortunately it is observed for only a very small number of substrate combinations [3]. The surface is usually not perfect during FM growth and may actuate in height over distances of tens or even hundreds of monolayers as a result of random impingement of atoms and two dimensional (2D) nucleation. However, thickness modulations or other indications of instability in the surface morphology are not present. On the other hand, the deposited material may aggregate into clusters which are located either on the bare substrate, the Volmer-Weber (VW) mode, or on top of a very thin, the Stranski-Krastanov mode [10]. The transition from the near-equilibrium at early stages to the kinetic models at the late growth occurs when the clusters reach a critical size. Modes of deposition are presented schematically in Fig. 1.
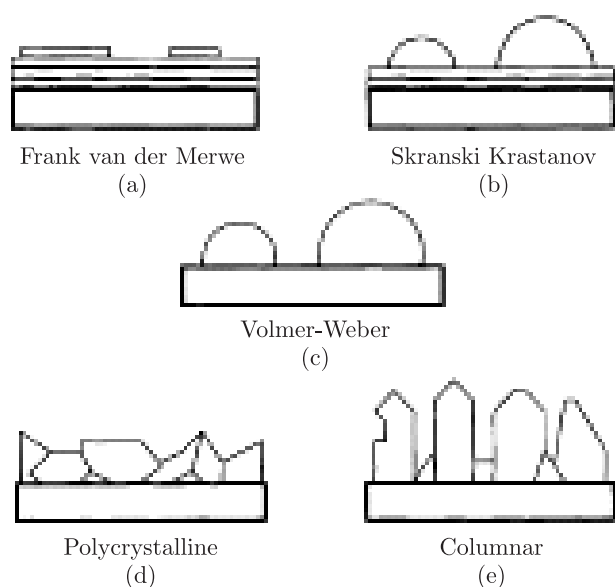

Fig. 1. Models of thin film growth (a), (b), (c) – early stages mechanism; (d), (e) – late mechanism

2. Experimental

2.1. Layer deposition and investigation. The layers were deposited using a pulsed Nd:YAG laser. Titanium targets were applied for ablation experiments. Laser system provides four beams of 1064 nm wavelength, 0.6 J pulse energy and 10 ns pulse duration at a repetition rate of 50 Hz [11]. In this multi-spot evaporation system, the targets are rotated during the laser irradiation in order to avoid the formation of deep craters. The

emitted species are deposited at room temperature (approximately 25°C) onto polyurethane substrates rotated during deposition. Cross section of the thin layer behaviour were investigated by transmission electron microscopy (TEM). Finite element modelling (FEM) based on the ADINA system was applied for modelling.

2.2. Results and discussion. Numerical model. Thin layers of TiN with the Ti interface deposited on the elastic polyurethane substrate were selected for theoretical investigations. The parameters and assumption of the materials are given in Table 1 and 2, respectively. Different nanoindenters were considered and their influence on the stress and strain distribution was calculated. The distance of the indenter movements was established to be 10nm. Titanium nitride (70 nm thick) with the titanium interface (16nm thick) deposited on the polyurethane substrate was taken for FEM. Four variants of nanoindenter tool were considered (Fig. 2). The nanoindenter diameters were close to those which would appear in the real application. The following tools with multiplication of 2 from 16 to 48 nm were used. Additionally, a sharp indenter with angle of 45° was considered. The influence of the "border" tools were analyzed, either, and contribution of the radius indenter to the behaviour of the layer were examined. The analyzed variants are presented in Fig. 2, schematically.

Table 1
Material parameters used in the FEM calculations

Material	Young´s modulus (GPa)	Poisons ratio	Material law
TiN (deposited layer)	616	0.25	Elastic-plastic bilinear. Initial Yield Stress $\sigma = 5000$ (MPa). Strain Hardening Modulus $E_H = 5000$ (MPa)
Ti (deposited layer)	116	0.3	elastic
Polyurethane (substrate)	4.420×10^{-3}	0.49	elastic
Nanoindenter			rigid structure

Table 2
Material assumptions for the temperature distribution calculation

	Substrate PU	Layer TiN
Initial temperature (°C)	20	30
Element group	Type 2D conduction planar	
Material properties	Thermo-isotropic	Thermo-plastic
Thermal expansion	$100 \times 10^{-6}/°C$	$9 \times 10^{-6}/°C$

The indentation process was simulated with the ADINA program. Two-dimensional calculations were chosen as a much more efficient than the three-dimensional ones, because of the lower mesh complexity. The calculated layer consisted of the

TiN external layer, and Ti interlayer. The mesh near the indenter and the interface layer has to be very fine to describe the deformation and stress distribution with sufficient accuracy. The specimen was represented by four node elements connected with each other (Fig. 3).
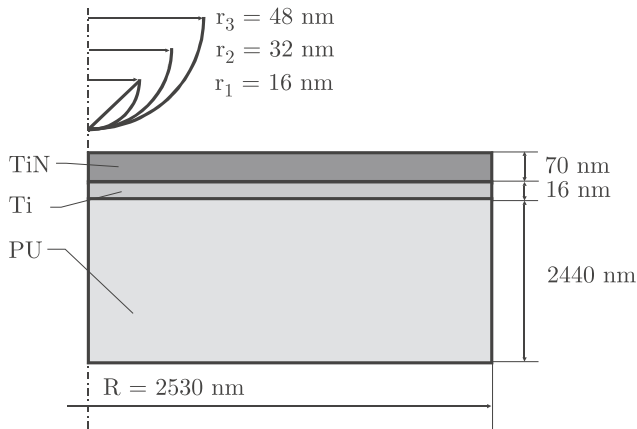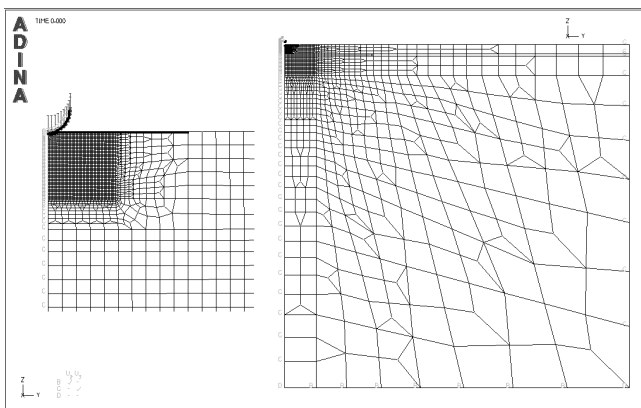

Fig. 2. Geometry of the analyzed variants

Fig. 3. FE mesh drawing of the TiN layer with the Ti interlayer on PU substrate

Main structure information:

— FEM model: axisymmetric, 4195 nodes, the total of 4142 elements in the main structure.
— 3 element groups:
  – Element group 1: 1020 axisymmetric solid elements. (PU)
  – Element group 2: 90 axisymmetric solid elements. (Ti)
  – Element group 3: 3032 axisymmetric solid elements. (TiN)
  – 1 contact surface group:
— Contact group 1: 2 axisymmetric 2D contact surfaces.

Nanoindentation verification test. On the basis of theoretical calculations the tribological test of nanoindentation was performed. The difference between the simulation and the experiment comes from the variation in the nanoindenter shape. Physical test was carried out along the respective procedure

along the Oliver & Pharr method of hardness measurement (No of norm ISO 14577-1, PN-EN ISO 6507-1). Main attention was focused on the elastic properties estimation of the material. The presented results concern an uncoated material (substrate) as well as material with the tested layer (Table 3).

Table 3
Results of tribological tests performed along the Oliver & Pharr method

Maximal load	Load rate	Unload rate	Results
Polimer substrate			
20.00 mN	40.00 mN/min	40.00 mN/min	Hv= 2.0723 Vickers H = 22.362 MPa E = 0.11834 GPa Poisson = 0.30
Polimer with layer			
5.00 mN	10.00 mN/min	10.00 mN/min	Hv= 17.016 Vickers H = 183.62 MPa E = 0.85353 GPa Poisson = 0.30
10.00 mN	20.00 mN/min	20.00 mN/min	Hv= 8.1639 Vickers H = 88.097 MPa E = 0.4594 GPa Poisson = 0.30
20.00 mN	40.00 mN/min	40.00 mN/min	Hv= 4.8382 Vickers H = 52.209 MPa E = 0.19806 GPa Poisson = 0.30

Applied strain. Strain was applied as a nanoindenter movement against the material. The average tool displacement was given in the level of four mesh elements.

Calculation of the indentation test. The displacement obtained for the round indenter is shown in Fig. 4, and for the sharp indenter in Fig. 8, respectively. The following results are presented:

— Strain distribution: Fig. 5 for the round indenter, Fig. 9 for the sharp indenter
— Stress distribution: Fig. 6 for the round indenter, Fig. 10 for the sharp indenter
— The area of plastic deformation: Fig. 7 for the round indenter, Fig. 11 for the sharp indenter

The results of the stress and strain distribution in the TiN layer and in Ti interlayer adherent to PU substrate is not taken under the main consideration. The key issue is to find an area of the crack endanger propagation in the layer.

The differences of the material behaviour were observed in the case of stress and strain distribution. The application of the round-shaped indenter resulted in lower values of the plastic deformation and in bigger reaction area than in the case of the sharp indenter. The typical edge for the plastic flow was calculated for the layer for which the parameters were simulated under the sharp indenter conditions. The strongest stress occurred near the indentation area as well as the plastic flow
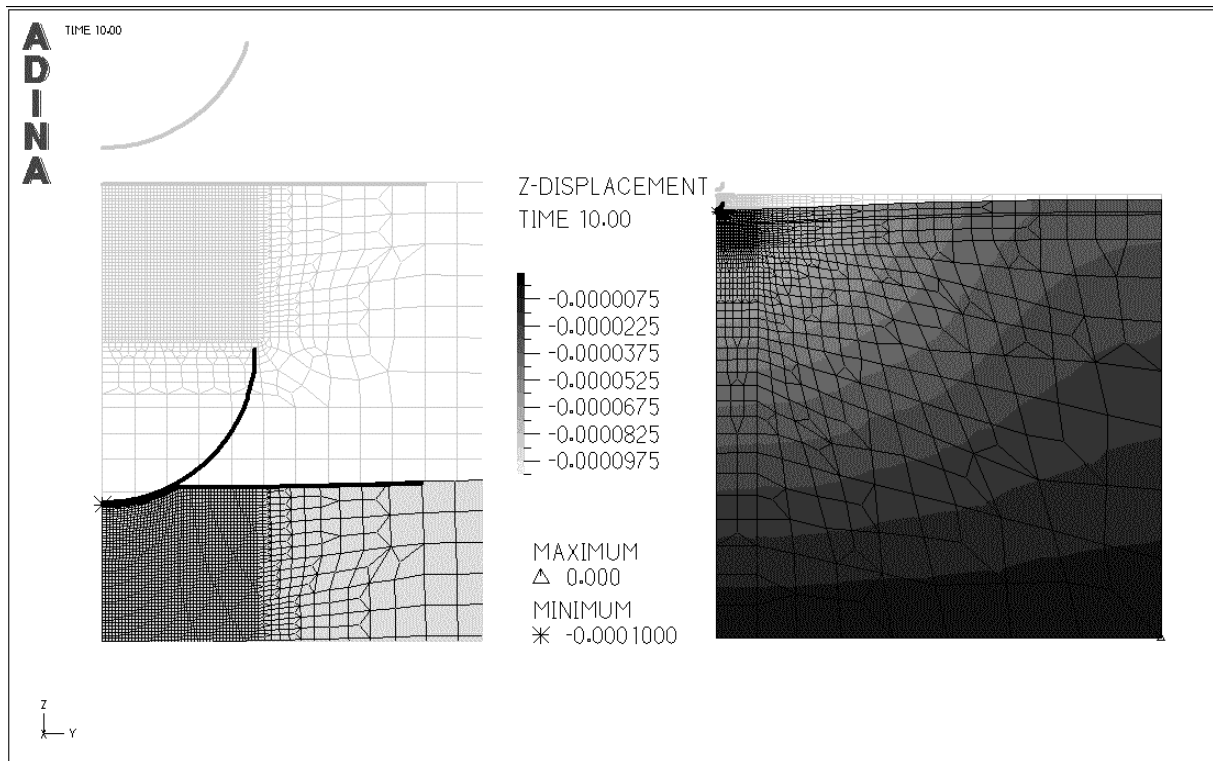
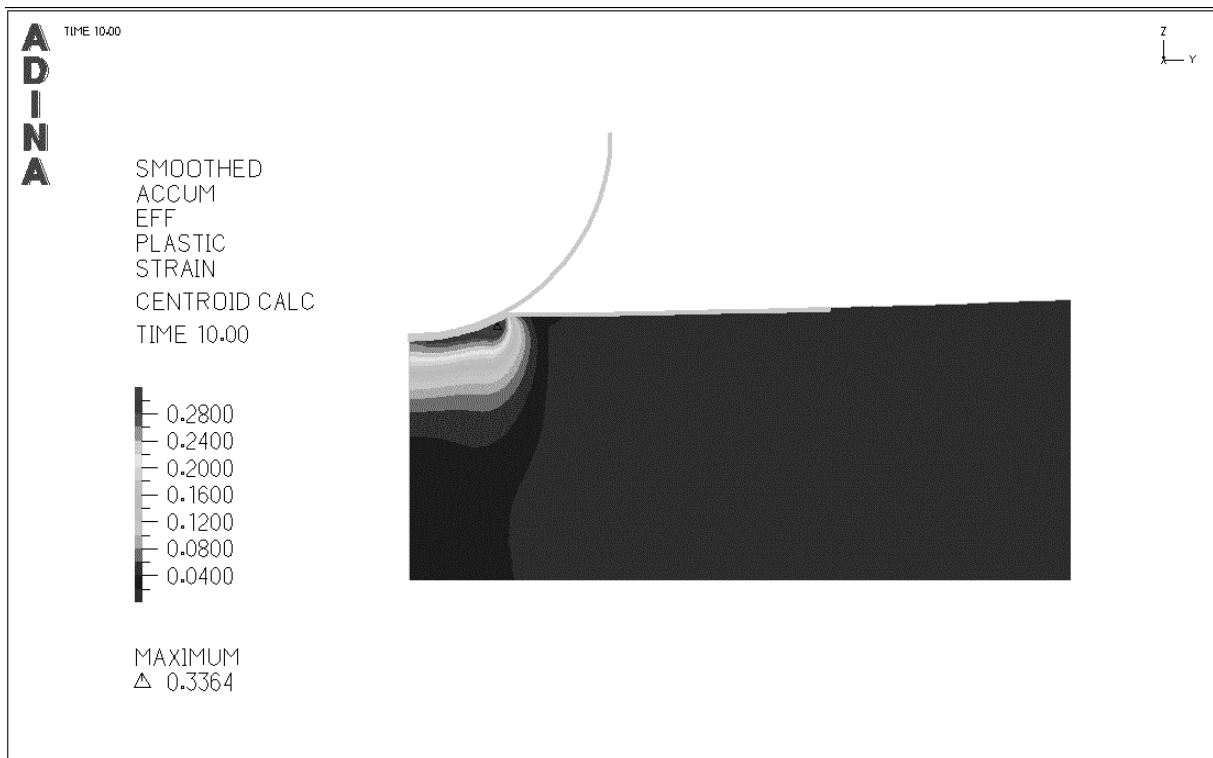Fig. 4. Displacement (mm) of the indenter into the layer for the round indenter $r_3 = 48$ nm

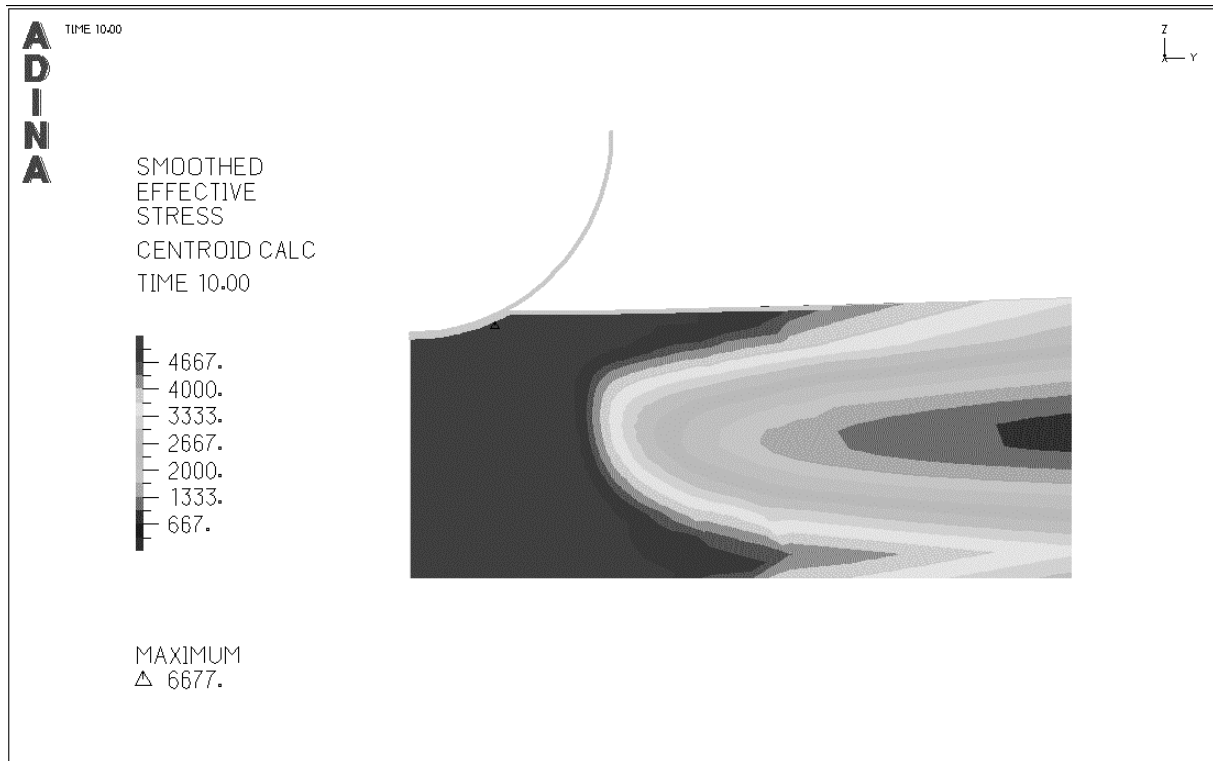Fig. 5. Plastic strain distribution in the TiN layer for the round indenter $r_3 = 48$ nm

Fig. 6. Effective stress distribution (MPa) in the TiN layer for the round indenter $r_3 = 48$ nm
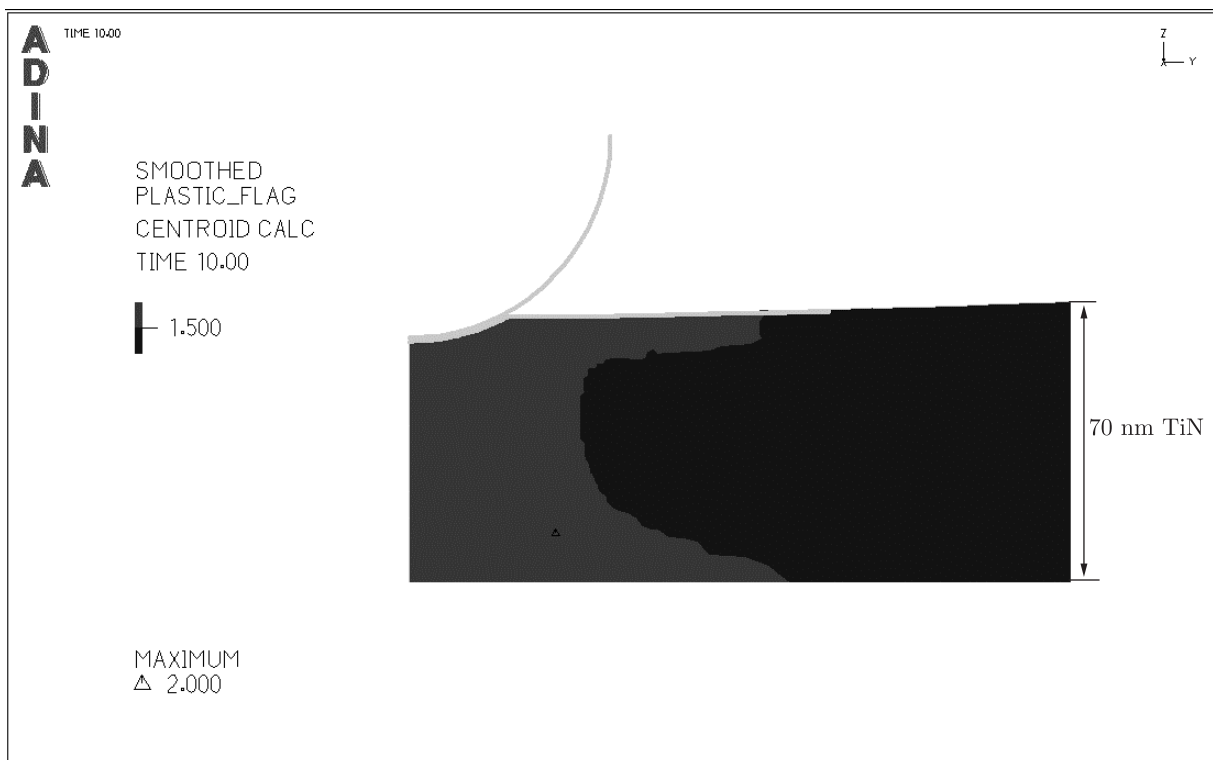

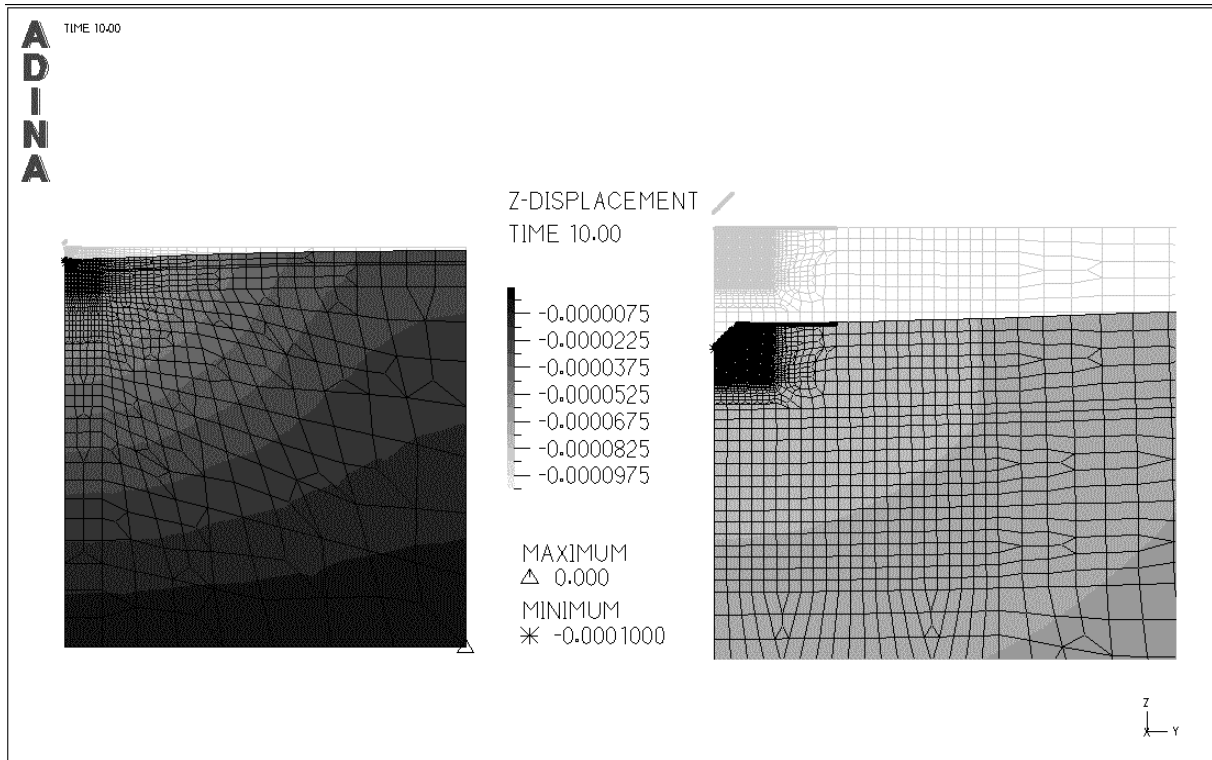Fig. 7. Area of the crack formation for the round indenter $r_3 = 48$ nm

Fig. 8. Displacement (mm) of the sharp indenter into the layer

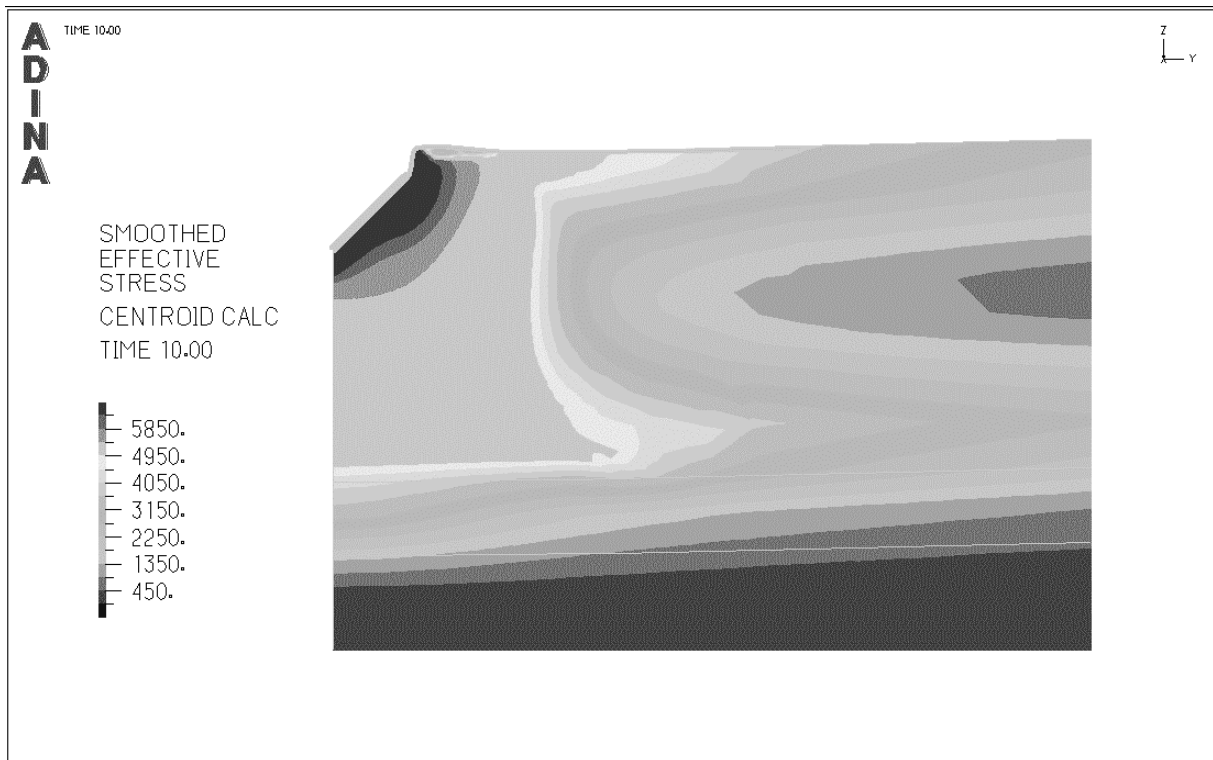Fig. 9. Strain distribution in the TiN layer for the sharp indenter

Fig. 10. Effective stress distribution (MPa) in the TiN layer for the sharp indenter

Fig. 11. Area of the crack formation for the sharp indenter

edge area. Figures 7 and 11 present the results of the crack formation in the endanger areas. They seemed to be similar to each other, and thus, the influence of both indenters on the crack appearance was similar as well.

The reason of such setup the tribological experiment was to calculate a possible effect which would occur in practical application. The main tribological properties were verified and established in the real experiment and the obtained results are presented in Table 3.

TEM microstructure of the TiN layers deposited on the PU substrate. The second part of the investigation considered the finite element modelling (FEM) application as a method for analysis of the physical phenomena observed in the microstructure studied by transmission electron microscopy (TEM). Furthermore FEM was used for a new layer composition prediction. The basis for the calculation was the temperature influence on the layer-substrate structure. The main assumptions comprise: slight temperature differences caused by the plasma, and its influence on the stress and crack formation. The microstructure of the cross section of the 250 nm thick layers of TiN deposited on polymer substrate is presented in Fig. 12. Deformation of the substrate during deposition, cracks and secondary nucleation of microcolumn from the crack area were found. Healing of cracks by increasing clustering of surface was observed. The microstructure of 250 nm thick layers was similar to the columnar model of growth (Fig. 1). Such structure is characteristic for brittle materials.
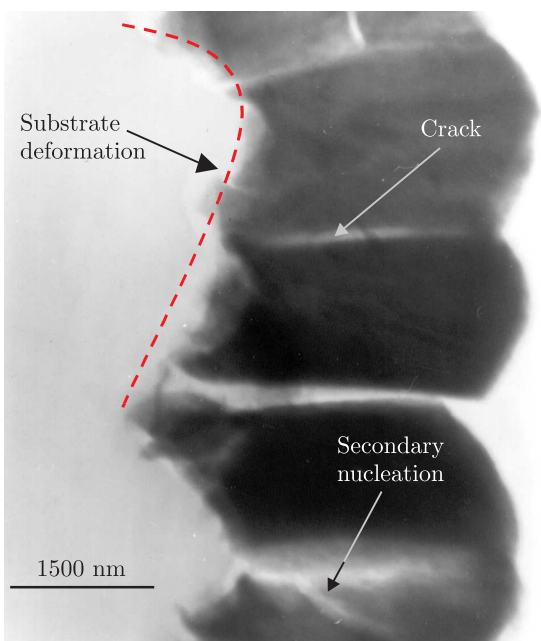

Fig. 12. TEM microstructure of cross section of 250 nm thick layer

The temperature distribution was estimated for slight temperature differences between the substrate and the layer (Fig. 13). The temperature increase was caused by plasma temperature as well as by transfer of kinetic energy onto the heat one. This could lead to slight temperature differences between the deposited layer and substrate. In spite of the temperature impact, there is no risk of substrate degradation. The model con-

sidered the subsequent sub-layer impact on the previous one. The main assumptions are given in Table 1.

(a)

Uniform temperature
distribution in the substrate
(b)

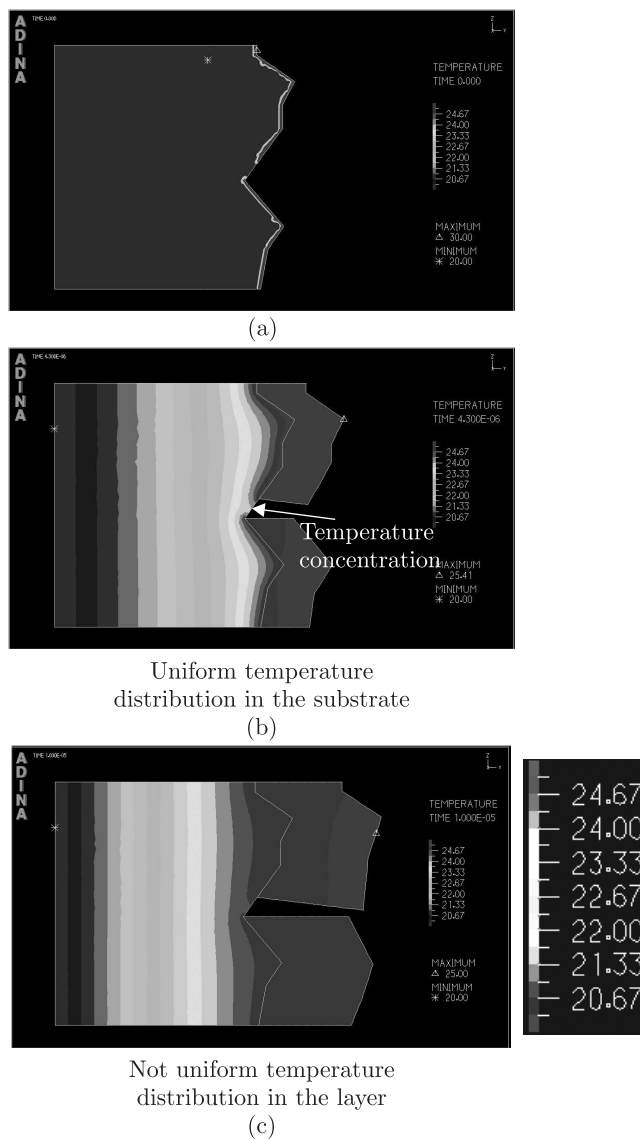Not uniform temperature
distribution in the layer
(c)

Fig. 13. Temperature distribution in the composition during deposition process; (a) initial stage, (b) medium stage, (c) late stage

Slight temperature concentrations were found especially in the areas of the cracks formation. The temperature propagation seemed to be disturbed by the substrate insulator. Even slight temperature differences could cause stress concentration, thus crack formation is possible due to the thermal expansion (thermal expansion for PU $100 \times 10^{-6}/°C$ and for TiN $9 \times 10^{-6}/°C$). Initial conditions were considered to be about room temperature. The heat energy which has an impact to the material comes from the kinetic energy of particles and from the heat transfer from plasma. This could lead to a slight temperature increase of material causing the temperature rise up to $50°C$.

The initial stage of the stress propagation appeared in the top parts near the substrate and followed to the surface. The direction of stress inclination, which could lead to the secondary nucleation, was also found (Fig. 14).
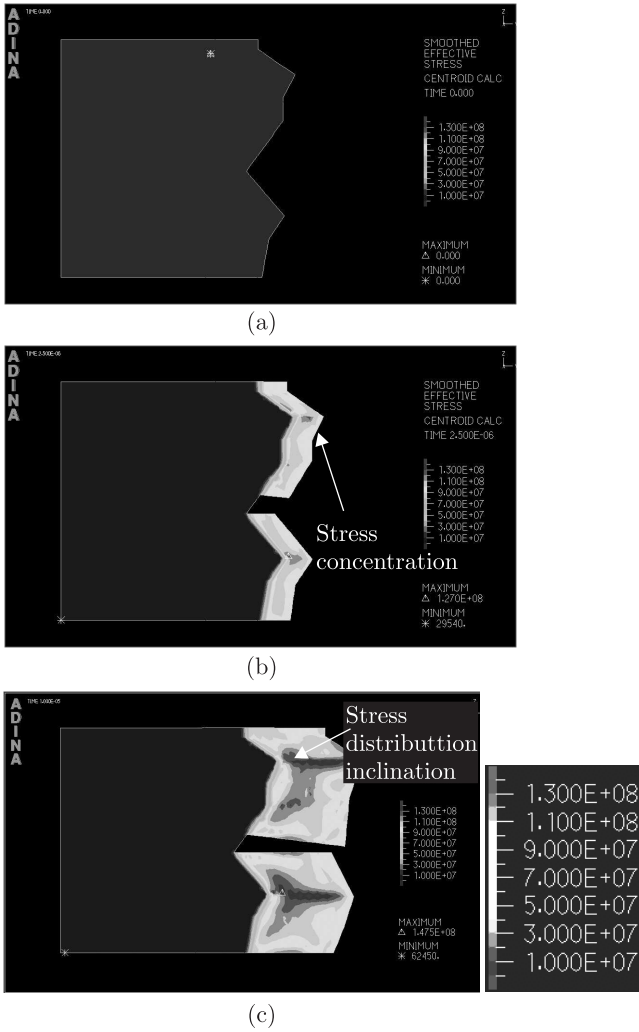
(a)

(b)

(c)

Fig. 14. The stress distribution in the composition caused by temperature; (a) initial stage, (b) medium stage, (c) late stage

(a)

(b)

Fig. 15. The temperature distribution in the composition during deposition process; (a) initial stage, (b) late stage

(a)

(b)

(c)

Fig. 16. The temperature distribution in the composition during deposition process; (a) initial stage, (b) 2D deposition, c) columnar deposition

On the basis of the previous experiences [8], diminishing of the layer thickness was suggested. FEM calculation was performed to estimate temperature distribution in the thinner layers. The uniform heat flow would not cause stress concentration, thus there is no serious endanger of the crack formation (Fig. 15). Homogeneous distribution of temperature occurred in the layers deposited with the 2D mechanism of film growth (Fig. 16). There is no concentration of temperature which could lead to stress propagation and crack formation. Thicker layers, deposited by the kinetic and columnar model could cause local temperature concentration.

Thin layers of 50 nm were deposited. TEM microstructure of cross section revealed good quality, lack of cracks and elastic behaviour (Fig. 17). On the basis of selected area electron diffraction pattern, the nanocrystalline structure was identified. It was possible to find places with a helical deformation occurred during the thin foils preparation using the "microtom" technique. No cracks and delaminations were observed.
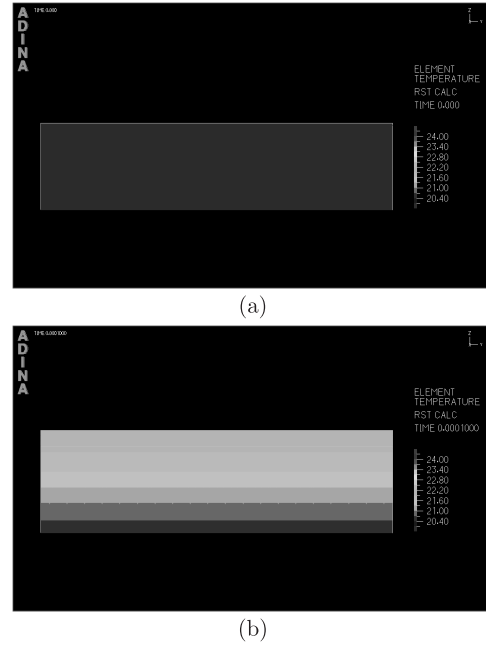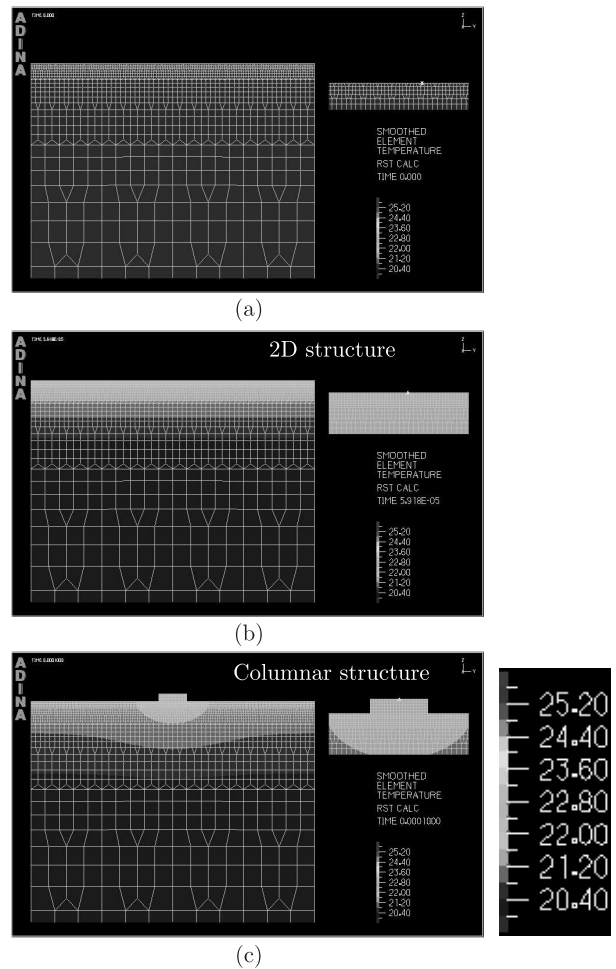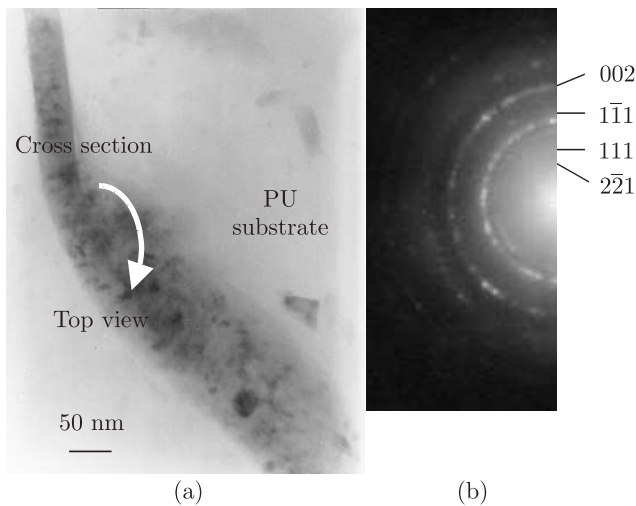
Fig. 17. 50 nm TiN layer deposited on PU substrate; (a) TEM micrograph, (b) selected area electron diffraction pattern

3. Concluding remarks

Differences were observed in the stress as well as strain distribution in respect to the applied thickness of the layer. They were dependent on the shape of the indenter. The formation of the elastic edge in the case sharp indenter was right. The finite element modelling presented in this paper does not consider reaction of molecules, however, in thin layers of thickness less than 100 nm, it could influence layer properties.

The second part of the work considered finite element modelling with the ADINA system as a method for interpretation of transmission electron microscopy results. On the basis of the result of calculations, a new layer composition was proposed. Layer thickness reduction caused elastic behaviour of the TiN layer. The study confirms successful PU modification with depositing of the TiN nano-layer which has nanocrystalline structure, is flexible, represents improve biocompatible, and well adhered to the polymer and could be applied in design of artificial heart implant [12] .

REFERENCES

[1] D. Rather, A.S. Hoffman, F.J. Schoen, and J.E. Lemons, Chapter 2, Classes of Materials Used in Medicine, *Biomaterials Science; An Introduction to Materials in Medicine*, 2nd editon; ed. B.D. Ratner, Elsevier Inc., 67–69 (2004).

[2] D.B. Chrisey and G.K. Hubler., *Pulsed Laser Deposition of Thin Films*, John Wiley and Sons, 1994.

[3] J.C. Miller and R.F. Haglund, *Laser Ablation and Desorption*, Academic Press, San Diego, vol. 30, 1998.

[4] B. Yin, W. Wang, and Y. Jin, The application of component mode synthesis for the dynamic analysis of complex structures using ADINA; *Computers & Structures* 5 (6), 931–938 (1997).

[5] K.J. Bathe, J. Walczak, and H. Zhang, "Some recent advances for practical finite element analysis", *Proceedings of the 9th ADINA Conference*, 511–521 (1993).

[6] D. Ma, K. Xu, and J. He, "Numerical simulation for determining the mechanical properties of thin metal films using depth-sensing indentation technique", *Thin Solid Films* 323, 183–187 (1998).

[7] G.H. Gilmer, H. Huang, and Ch. Roland, "Thin film deposition: fundamentals and modelling", *Computational Materials Science* 12, 354–380 (1998).

[8] R. Major and P. Lacki, "Finite-element modelling of thin films deposited on the polyurethane substrate", *Archives of Metallurgy and Materials* 50, 379–385 (2005).

[9] M. Bienfait, J.L. Seguin, J. Suzanne, E. Lerner, J. Krim, and J.G. Dash, *Phys. Rev.* B 29, 983 (1984) in: J.M. Olson, A.E. Blakeslee, M.M. Al-Jassim (eds.), *Crystal Properties and Preparation*, vol. 21, Trans. Tech. Publications, Switzerland, 59 (1989).

[10] J.A. Venables and G.L. Price, in: J.W. Matthews (ed.), *Epitaxial Growth*, Part B, Academic Press, New York, 1975.

[11] B. Major, W. Mróz, T. Wierzchoń, W. Waldhauser, J.M. Lackner, and R. Ebner, "Pulsed laser deposition of advanced titanium nitride thin layers", *Surf. Coat. Technol.* 180–181, 580–584 (2004).

[12] R. Kustosz, R. Major, T. Wierzchoń, and B. Major, "Designing a new heart", *Academia* 3, 14–17 (2004).